ACOUSTICS 2012

# Quantitative linear and nonlinear resonant inspection techniques for characterizing thermal damage in concrete

C. Payan[a], T.J. Ulrich[b], P.-Y. Le Bas[c] and M. Guimaraes[d]

[a]Aix-Marseille Univ, LCND, IUT Aix en Provence, 413 Av. Gaston Berger, 13100 Aix en Provence, France

[b]Geophysics Group, Los Alamos National Laboratory, Los Alamos, Los Alamos (NM), 87544, USA

[c]Earth and Environmental Sciences, Los Alamos National Laboratory, MS D443, Los Alamos, NM 87545, USA

[d]Electrical Power Research Institute, Charlotte, Charlotte, 28262, USA

cedric.payan@univ-amu.fr

In the context of license renewal in the field of nuclear energy, maintaining in service and re-qualifying existing concrete structures for the period of long term operations is challenging. The integrity of concrete in the concrete pedestal and biological shield wall in nuclear plants remains unknown. These structures have been subjected to radiation and medium temperature for a long period of time. This paper aims at providing some quantitative information related to the degree of micro-cracking of concrete and cement based materials in the presence of thermal damage. We develop a methodology based on linear resonant ultrasound spectroscopy, numerical simulations and nonlinear resonant ultrasound spectroscopy to provide quantitative values of nonlinearity. We show the high sensitivity of derived nonlinearity to thermal damage and its correlation with the evolution of concrete microstructure.

# 1 Introduction

Mechanical resonance is a phenomenon that occurs when the wavelength λ corresponds to a characteristic dimension (or a multiple) of a sample. For simplification, we consider here a quasi-1D problem, a cylinder of length L with a Young's Modulus E. If this cylinder is driven at a specific frequency f0 for which the half wavelength equals L, the resonance is reached (Fig. 1).

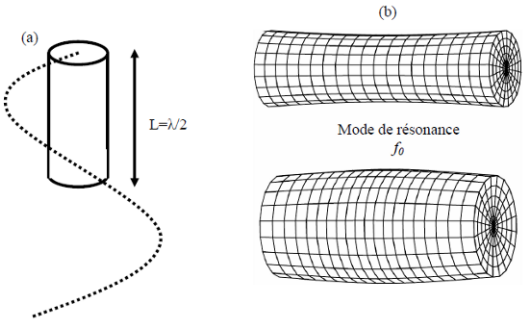


Figure 1: Resonance mode of a cylinder. (a) wavelength compared to the length of the sample. (b) resonance mode

As the speed of sound s is linked to the Young's modulus E as $s=\sqrt{(E/\rho)}$ and that $\lambda=s/f_0$, one can extract the relationship :

$$f_0 = \frac{1}{2L}\sqrt{E/\rho} \quad , \qquad (1)$$

where ρ is the density. So, as the length and the density are known, by measuring the resonant frequency one can evaluate the elastic properties (E).

Based on this simple principle, but adapted to more complex 3D geometries, resonance inspection techniques are known and employed for years [1]. Resonant Ultrasound Spectroscopy (RUS) allows the material elastic properties to be determined accurately by non-destructive means. The input values are the sample geometry and the density. By exciting the sample in a large frequency range, one can extract the resonance peaks (experimentally measured values) corresponding to various eigenmodes. Then, by combining experimental and input values, an inversion algorithm provides the full elastic tensor of the sample. This can apply to any elastic material type (isotropic or anisotropic). RUS has been employed in various homogeneous materials and more recently in inhomogeneous ones such as rocks [2] cement [3]. However, this method has never been employed for concrete nor to detect damage. Our concrete samples have a finite geometry (parallelepiped) making the RUS method a perfect candidate to determine their linear characteristics.

Nonlinear Resonance Ultrasound Spectroscopy (NRUS) was developed at LANL in the 1990's. It exhibits a large sensitivity to damage in a wide range of micro-inhomogeneous materials for various application domains (concrete, rocks, damaged steel or aluminum components, damaged composite, bones, etc.). The nonlinear parameter is usually extracted by the slope of the line (Fig. 2) by

$$\frac{f - f_0}{f_0} = \alpha \Delta\varepsilon \quad , \qquad (2)$$

where $f_0$ is the linear resonance frequency (low amplitude), $f_i$ the resonance frequency when drive at the $i_{th}$ amplitude, α the nonlinear parameter and Δε the strain amplitude. Since this method is applied to samples with appropriate geometry (cylinder with large aspect ratio), as the vibration mode along its height is very easy to detect, the measured vibration amplitude of the sample is proportional to the strain. However, for more complex geometry, this assumption does not hold because of the mode shapes complexity (Fig. 6). This is why we make use of numerical simulation that allows identifying a particular mode and so extract the strain values. The input values of numerical simulation are the elastic constants provided by RUS measurements.

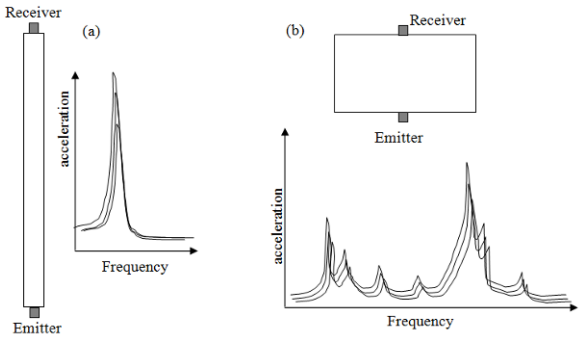


Figure 2: Resonance mode of a cylinder. (a) wavelength compared to the length of the sample. (b) resonance mode

It is important to notice that this procedure is followed in order to get quantitative values of nonlinearity, which has never been done yet for particular geometries. To detect damage, even qualitatively, these steps are not needed. This point is underlined at the end of the document.

The following sections describe RUS measurements, how these results are integrated to numerical simulations and NRUS results.

## 2 Thermal damage process of concrete

Concrete is a complex multiphase solid material composed, before curing, of anhydrous cement, aggregates, sand and water. Anhydrous cement is principally composed of Silica (SiO2), Alumina (Al2O3), Lime (CaO) and Calcium Sulphate (CaSO4). The aggregate size is generally between 3 and 25 mm. Cohesion of concrete is guaranteed by a water cement ratio (w/c) of typically 0.3<w/c<0.6. Chemical processes occur with heat generated during curing, producing an increase of porosity and micro-cracks.

In concrete the most brittle zone is the interface between aggregates and cement paste. This zone, namely the transition halo, is the most porous and crystallized one. The presence of silica fume and/or plasticizer in high performance concrete reduces the porosity in this zone. With increasing temperature, this zone is progressively degraded due to the evaporation of free water and mainly to the differential dilation between aggregates (expansion) and cement paste (shrinkage).

Chemical reaction occurring with thermal damage process of concrete is known and synthesized in Tab. 1. Evidence of cracking is obtained applying macrography (Fig. 3). It reveals two essential observations: (i) There is no preferential cracking direction validating our hypothesis of isotropic damage; (ii) Most cracks appear at the cement-aggregate interface (transition halo) and in the cement matrix but never inside the aggregates, following the chemical process described in Tab. 1 (the first aggregate transformation appears at 600 °C).

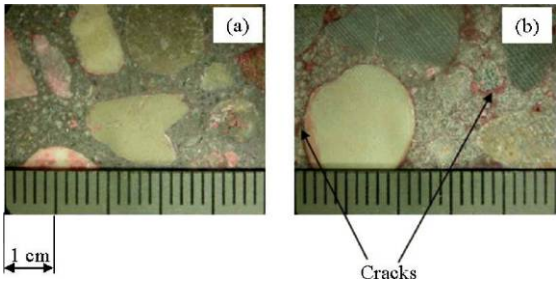


Figure 3: Resonance mode of a cylinder. (a) wavelength compared to the length of the sample. (b) resonance mode

Table 1: Chemical process occurring in concrete while increasing temperature. The top three lines are the temperature range studied here.

| | |
|---|---|
| →105 °C | « Free » water evaporation |
| →300 °C | First step of dehydration. Breaking of cement gel and uprooting of water molecules into hydrated silicates. |
| 400→500 °C | Portlandite decomposition : $Ca(OH)_2$ → $CaO+H_2O$ |
| 600 °C | Structural transformation of quartz α into β - swelling of quartziferous aggregates |
| → 700 °C | Second dehydration step : dehydration of Hydrated Calcium Silicates |
| → 900 °C | Limestone decomposition : $CaCO_3$ → $CaO+CO_2$ |
| 1300 °C | Aggregates and cement paste fusion |

## 3 RUS measurements

Each sample is placed on a stand with various position to pick the entire set of resonance modes needed for the RUS inversion. One of the 3 transducers (Fig. 4) is driven by a sinusoidal voltage, onto a given frequency range, while the two others record the response. The sample is oriented in various positions in order to be able to pick each of the first 10 resonance frequencies. For this study, 10 resonant frequencies (Fig. 5) are used to get the linear elastic characteristics of the sample (i.e., compressional and shear moduli C11 and C44, which can be related directly to E and ν).

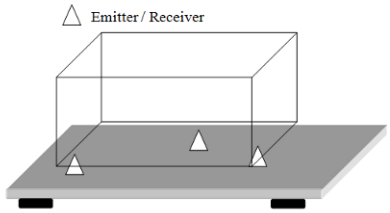


Figure 4: Resonance mode of a cylinder. (a) wavelength compared to the length of the sample. (b) resonance mode

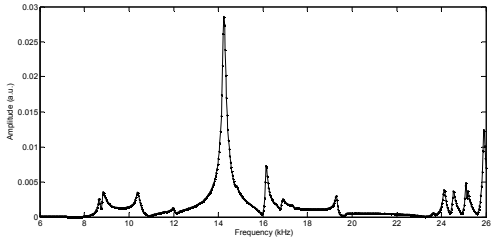


Figure 5: Resonance mode of a cylinder. (a) wavelength compared to the length of the sample. (b) resonance mode

The 10 firsts resonance frequencies determined, the inversion procedure provide the elastic characteristics given Table 2. These experiments have been performed and processed using the RITA software developed at LANL.

Table 2: RUS derived elastic properties of the samples. E : Young Modulus and ν : Poisson ratio.

| | E (Mpa) | ν |
|---|---|---|
| HPC | | |
| 20 | 48901 | 0.21 |
| 120 | 45342 | 0.19 |
| 250 | 40199 | 0.22 |
| 400 | 24782 | 0.10 |
| OC | | |
| 20 | 36942 | 0.20 |
| 120 | 35492 | 0.18 |
| 250 | 28565 | 0.13 |
| 400 | 16396 | 0.08 |
| M | | |
| 20 | 37176 | 0.17 |
| 120 | 38434 | 0.17 |
| 250 | 33588 | 0.14 |
| 400 | 26509 | 0.09 |

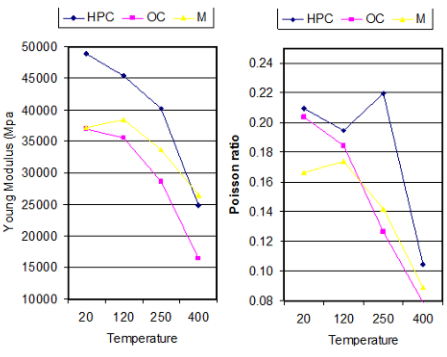


These values highlight the effect of thermal damage on concrete with a decrease of elastic properties with increasing damage. As expected, High Performance Concrete have better mechanical properties than Ordinary Concrete and Mortar suffers in a lesser extent from thermal damage because of the absence of aggregates, and thus a transition halo. These results are in agreement with existing literature [4].

To compare these results with standard non-destructive testing procedures in concrete, we performed wave speed measurements. The results are compiled in the next section.

# 4 Wave speed measurements

These measurements were performed at various frequencies with a standard zero crossing method (the first signal point getting out of the noise is supposed to represent the time of flight). We tried 3 frequencies, 60, 250 and 500 kHz, to highlight the effect of multiple scattering of acoustic waves in concrete. This multiple scattering is due to the presence of aggregates that diffuse the energy in every direction during wave propagation. The measured pressure wave speeds are given in Fig. 6a for concrete samples. The measured wave speed, that can be used to evaluate the linear elastic properties, depends on the frequency employed for measurements, which is not physically possible. It means that standard procedures for wave speed measurements are able to catch an evolution of wave speed while the frequency and the aggregates (responsible for multiple scattering) remain the same over the measurements. It is not possible to link these wave speeds with the elastic modulus, which is obvious when comparing wave speeds measured from pulse arrivals versus the wave speeds extracted from RUS. The same procedure is applied to a Plexiglas sample (Fig. 6a), which is homogeneous. In this sample the wave speed remains constant for every frequency.

We also compare (Fig. 6b) the elastic properties ($C_{11}$ = $\rho * s^2$) derived from RUS and the present wave speed measurements for the OC20 sample.

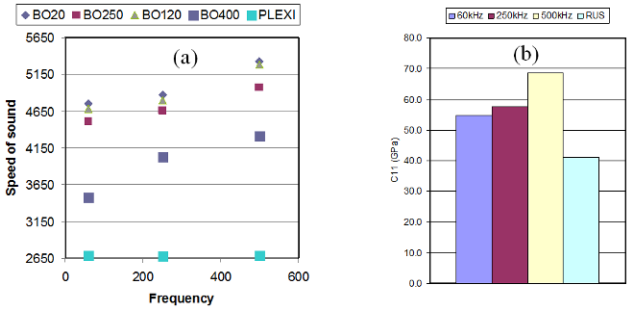


Figure 6: (a) Evolution of the compressional wave speed as a function of frequency in concrete samples. (b) Elastic constant derived from RUS and wave speed at various frequencies (OC20 sample).

# 5 Nonlinear Resonance Ultrasound Spectroscopy

Nonlinear acoustics based NDT methods are now used to detect damage in various fields. They exhibit a sensitivity to damage often orders of magnitude higher than standard linear parameters such as pulse wave velocity. In concrete, many studies highlight these methods as promising for many applications, such as macro-crack detection [5], mechanical damage [6], the effect of water saturation [7], thermal damage [8], carbonation assessment [9], ASR detection [10]. However, most of these studies are qualitative and only relate the effect of damage (or environment) on the variation of the nonlinear parameter. We purpose here to provide quantitative values of the nonlinearity compared to the evolution of concrete microstructure.

For NRUS studies, a transducer able to drive the sample at high amplitude is needed. We choose an ultrasonic cleaning transducer driven by an amplifier to a peak voltage of 200V. The laser vibrometer records the velocity at the sample center. The RITA software developed at LANL has been employed for the data acquisition and analysis. It allows generating signals at various amplitudes and frequencies, and analyzing the resonance curves. The experimental scheme is presented Fig. 7.

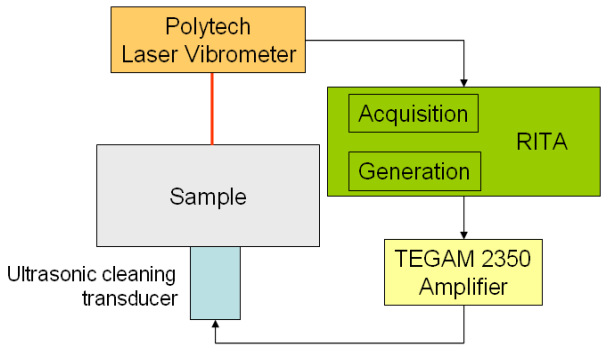


Figure 7: NRUS experimental scheme

To become quantitative, we need to select a resonance mode that will remain the same mode shape for each sample (e.g., a bulk "breathing" mode). In addition, it has to be selected with the maximum strain amplitude that can be reached for this particular geometry, because the nonlinearity is driven by strain amplitude (Eq. 2). To select this mode, we drive the samples at low amplitude (Fig. 8). Two high amplitude modes appear : (i) mode 1 marked by a large point and (ii) mode 2 in the highlighted region.

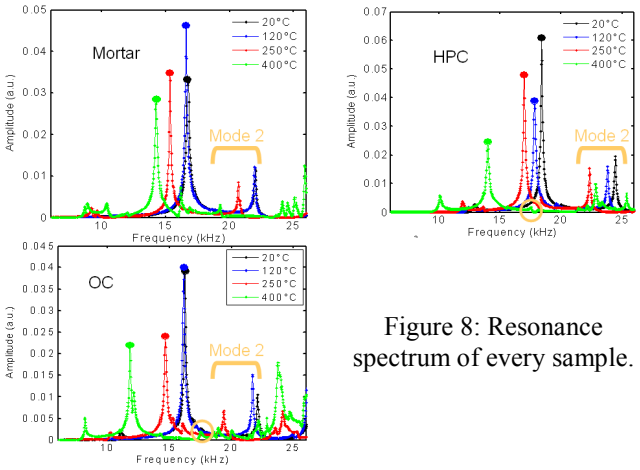


Figure 8: Resonance spectrum of every sample.

Most quantitative studies would have chosen the highest amplitude mode, i.e. mode 1. As we have the linear elastic characteristics of the samples (obtained from RUS), we use them as input for numerical simulation using Comsol. We model the experiments with the exact geometry, an additional mass (representing the transducer), and the laser spot that records the out of plane velocity at the top of the sample (Fig. 9).

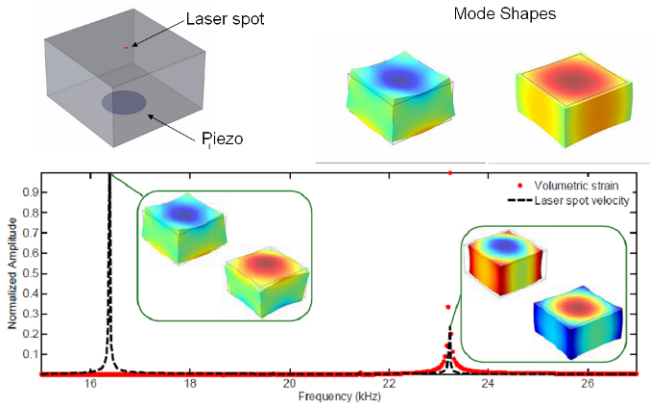


Figure 9: Numerical simulation of experiments.

One can realize that the highest velocity amplitude (black dashed curve) mode is a nearly zero volumetric strain (red dotted curve) amplitude mode because of the symmetry of the mode shape. The second mode, reaches a high strain amplitude with a low velocity at the top of the sample (laser spot location). The study of low volumetric strain mode may be of interest from a basic research point of view because of domination of shear effects, but this is not the purpose of this study. So, we select the "bulk mode" corresponding to an analogous mode as for cylinders (Fig. 1) that will allow obtaining quantitative values of the nonlinearity. Then, the same procedure is applied to each sample to get the absolute value of the volumetric strain so as we are able to link the measured velocity (laser) to the strain inside the sample.

With the mode selected, NRUS measurements are performed for each sample. The results are given in Figs. 10 to 12 for, respectively, Mortar, High Performance Concrete and Ordinary Concrete. The slopes of the lines are the nonlinear parameter α evaluated from Eq. 2.

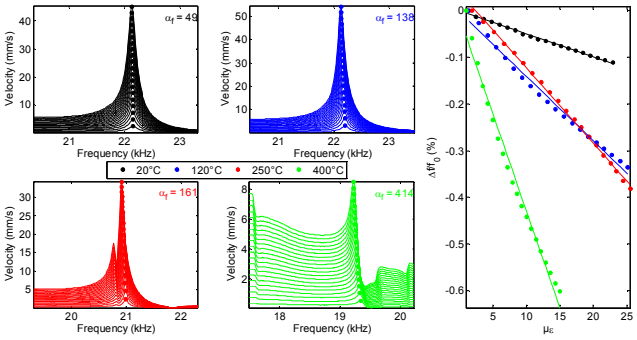


Figure 10: Mortar NRUS results.

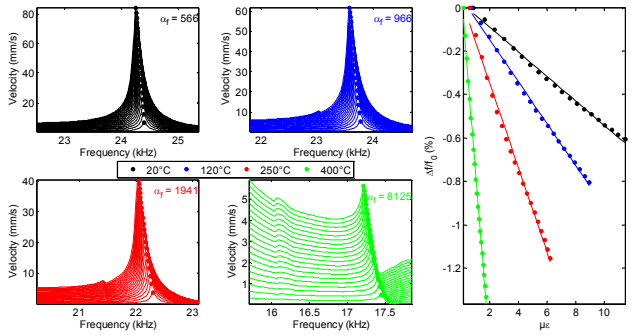


Figure 11: High Performance Concrete NRUS results.

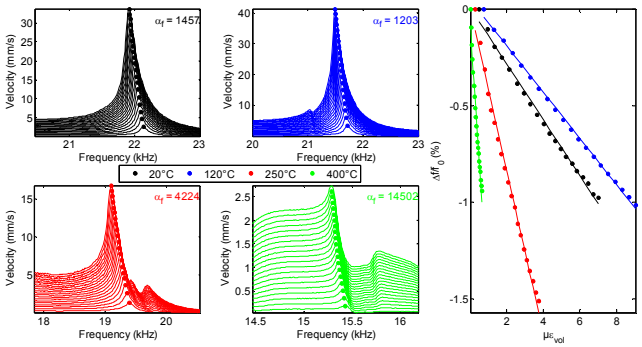


Figure 12: Ordinary Concrete NRUS results.

We can observe from these plots that 120°C and 250°C damaged Mortar samples have a similar nonlinearity, as well as 20°C and 120°C Ordinary Concrete ones. However, for each sample set, the variation amplitude is one order of magnitude (10 times higher at 400°C than 20°C). It is important to notice that without taking into account the true strain inside the sample, the net effect appears larger. This is explained by the decrease of the elastic properties that has to be taken into account. For a given amplitude level σ, as the modulus E decreases with damage, the strain ε inside the sample is higher (σ = E ε), so the slope decreases.

The linearity of the experimental system has been checked by applying NRUS to a known linear material (plexiglass) (Fig. 12) with the same geometry as the concrete samples and thus exhibiting the same resonance mode shapes. The lower frequencies of these modes simply indicate that the plexiglass is a softer material than the concrete.

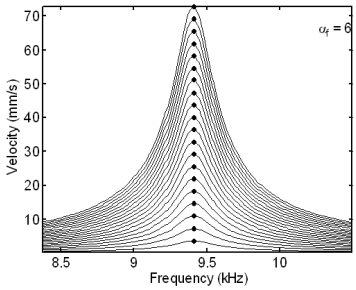


Figure 12: Plexiglass sample NRUS results

# 6 Summary-Conclusion

The compilation of linear and nonlinear results is given Fig. 13. The linear parameter chosen is the speed of sound calculated from RUS measurements. We use this linear indicator to compare with nonlinearity because the frequency shift, and so α, and speed of sound are comparable in terms of units. In addition, speed of sound is a standard NDT indicator. To compare with elastic modulus, further study on nonlinearity is needed to directly link the nonlinearity and the elastic properties change with increasing amplitude. Such a basic research topic is underway.

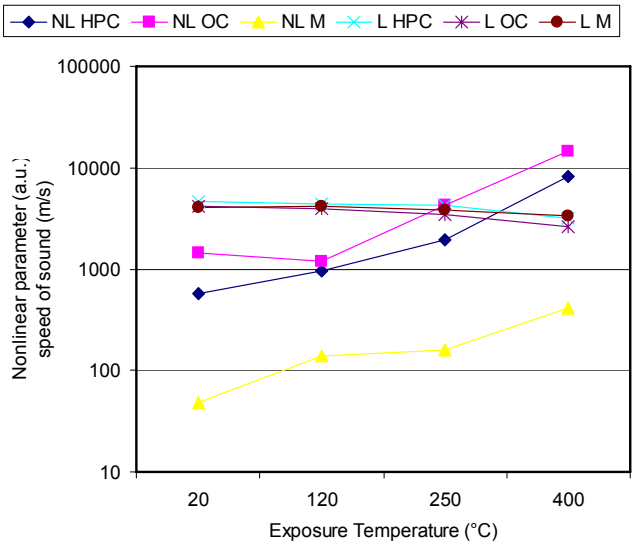


Figure 13: Compilation of linear (L : speed of sound) and nonlinear (NL : nonlinear α parameter).

As expected, these results reveal a great sensitivity (two orders of magnitude higher) of the nonlinear parameter to thermal damage as regarded with a standard linear NDT indicator (speed of sound). As stated in section 2, most of the damage comes from the transition halo (aggregate/cement interface). Thus, while there is no aggregate inside, the Mortar samples are less nonlinear than the other concrete samples. Of all the samples, Ordinary Concrete is more nonlinear than High performance concrete due to the presence of silica fume and plasticizer in HPC that reduces the porosity at the transition halo.

This is the first time in the literature that the combination of linear measurements (RUS) with numerical simulation and nonlinear measurements (NRUS) allows to quantitatively evaluate the nonlinear behavior of materials. It is applied to study the effect of thermal damage in concrete with results correlated to the evolution of the microstructure.

# References


[1] Migliori A., John L. Sarrao, Resonant ultrasound spectroscopy: applications to physics, materials measurements, and nondestructive evaluation, Wiley, 1997

[2] Ulrich, T.J., McCall, K.R., and Guyer, R.A., Determination of elastic moduli of rock samples using resonant ultrasound spectroscopy, J. Acoust. Soc. Am. 111(4), 1667-74 (2002)

[3] Wu W. et al., Measurement of Mechanical Properties of Hydrated Cement Paste Using Resonant Ultrasound Spectroscopy, Journal of ASTM International, Vol. 7, No. 5 (2010)

[4] Maréchal, JC. Variations of the modulus of elasticity and Poisson's ratio with temperature. In Concrete for Nuclear Reactors, ACI SP-34, 1, 495-503 (1972)

[5] Zardan J.-P., C. Payan, V. Garnier and J. Salin, Effect of the presence and size of a localized nonlinear source in concrete, Journal of the Acoustical Society of America 128 (1), EL38-EL42 (2010)

[6] Antonaci P, C L E Bruno, A S Gliozzi, M Scalerandi, Monitoring evolution of compressive damage in concrete with linear and nonlinear ultrasonic methods, Cement and Concrete Research 40 (7), 1106-1113 (2010)

[7] Payan C., V. Garnier and J. Moysan, Effect of water saturation and porosity on the nonlinear elastic response of concrete, Cement and Concrete Research 40, 473–476 (2010)

[8] Payan C., V. Garnier, J. Moysan and P. A. Johnson, Applying nonlinear resonant ultrasound spectroscopy to improving thermal damage assessment in concrete, Journal of the Acoustical Society of America 121 (4), EL125-EL130 (2007)

[9] Bouchaala F., C. Payan, V. Garnier and J.P. Balayssac, Carbonation Assessment in Concrete by Nonlinear Ultrasound, Cement and Concrete Research 41, 557–559 (2011)

[10] Kodjo A et al., Evaluation of damages due to alkali-silica reaction with nonlinear acoustics techniques, POMA 7, 045003 (2009)